

# ***THE NEW COUPLED TSM FOR THE 3-D***

## ***BEAM-COLUMN ELEMENTS***

By K. F. Sideek,<sup>1</sup> and S. Z. AL-Sarraf<sup>2</sup>

### **ABSTRACT**

A new coupled TSM is presented which includes the geometrical non-linearity effects of axial deformation, shear deformation, flexural and shear bowing, change in geometry and the axial force influence on the member torsional stiffness. The TSM derivation also takes into account the twisting moments influence on the axial deformations (the new 3-D or twisting effect), the fixed end actions (FEA.) and finally the special causes (temperature, lack of fit, initial imperfection, support yielding, etc.) is derived and presented. The computational technique and the computer program (*NASCFI*) algorithm are detailed.

A method for large deformation and stability analysis of elastic space frame based on Eulerian approach with five types of Newton-Raphson load control iterational-incremental technique is adopted. Local member force-deformation relations are based on the beam-column approach taking into account large joint translations and rotations. For the beam-column case studies, *NASCFI* shows good agreement of the new approach with exact Elastica solution of problems or with the experimental problems. By including new effects of both the flexural-shear bowing and the 3-D, the present work indicates a significant amount of difference with other research results of similar problems. The new twisting effect has a major role that relates the axial deformation with the shear effect acting transversely.

---

<sup>1</sup> Dr. K. F. Sideek, Building & construction Department, University of Technology, Baghdad-Iraq...

Personal E-mail: [drkhfaldy@yahoo.com](mailto:drkhfaldy@yahoo.com).

<sup>2</sup> Prof. Dr. S. Z. Al-Sarraf, Building and Construction Engineering Department, University of Technology, Tel-Muhamad, Baghdad-Iraq.

Key words: axial shortening, , axial stiffness, bowing, flexural – torsional buckling, large-deformation, non-linearity, shear deformation, stability, stiffness matrices, torsional stiffness.

## **1- Introduction**

The stability, the flexural-shear bowing, the new twisting functions and the FEA including shear effect which are presented elsewhere[14], give a new performance of the TSM of 3-D beam-column element. The large deflection theory requires a great deal of time and effort in order to get as close as possible to the exact Elastica. Experimental and theoretical 2-D and 3-D investigations were studied by many researchers (using beam-column, finite element or discrete field methods as analytical procedures) for both the small deflection (SD) and the large deflection (LD) beam-column theories. Researches were made by Livesly (1956), Renton (1962), Saffan (1963), Merchant (1966), Conner et. al. (1968), Jennigs (1968), Haisler et. al. (1972), Oran (1973), Vinnakota & Aysto (1974), Oran & Kassimali (1976), Wood & Zienkiewicz (1979), Bridge (1979), Fujii (1983), Kassimali (1983), El-Zanaty et. al. (1983), Wen & Rahim Zadeh (1984), See & Mconnel (1986), Al-Sarraf (1986), Hsaiao & Hau (1987), Kam (1988), Meek & Loganathen (1989), Al-Bermani & Kitipornchai (1990), Sideek (1990), Kassimali & Abbasnia (1991), Kauthia (1992), Al-Sedder (1994), Sideek (1995), Sully & Hancock (1996), and many others.

Saffan[13], was the first who stated the analytical procedure of linearized incremental TSM of conventional beam-column theory that this work adopts for analysis. Further 3-D developments were made by Oran [11&12], Oran and Kassimali[10], Kassimali[7] and last but not least Kassimali and Abbasnia[8].

## **2- The new TSM build-up**

The new twisting functions presented elsewhere[14] gives a new derivation of this procedure to include the coupled torsional-flexural action. The special effects of temperature, lack of fit, initial imperfection, (axial, flexural), initial angle of twist and support yielding in all DOF is treated as FEA to be added to the member local forces vector in the corresponding direction and DOF of each effect. This means that each effect has its own contribution in the non-linear analytical operation during each incremental-iterational loop. These special FEA effects can be

found in text books[6&14]. These actions are put in vector form and added to the applied load vector of the element so the equilibrium equation of the B-C element can be written as: -

$$\{F\} = [t].\{u\} \dots\dots\dots(1)$$

Where  $\{F\}$  is the force vector of the element in local coordinates and  $\{u\}$  is the deformation vector of the element in local coordinates.

The present work adopts the same procedure presented by Oran[12], and Kassimali & Abbasnia[8]. Thus references [8&12] are utilized for the joint displacement, the member orientation matrix, the relative deformations and the basic member force-deformation relations.

The New 3-D Coupled TSM: In the present work a complete interaction between twisting angle ( $\phi$ ) and rotations ( $\theta_1$  &  $\theta_2$ ) occurs, so the coupled TSM can be now built up, since: -

$$t_{ij} = \frac{\partial s_i}{\partial u_j} + \frac{\partial s_i}{\partial \rho} \frac{\partial \rho}{\partial u_j} \text{ for } (i, j = 1 \text{ to } 6) \dots\dots\dots(2)$$

Where :-

$$\begin{bmatrix} S_1 = M_{13} \\ S_2 = M_{23} \\ S_3 = M_{12} \\ S_4 = M_{22} \\ S_5 = M_t \\ S_6 = QL \end{bmatrix} = (\text{force vector}), \begin{bmatrix} u_1 = \theta_{13} \\ u_2 = \theta_{23} \\ u_3 = \theta_{12} \\ u_4 = \theta_{22} \\ u_5 = \phi \\ u_6 = \frac{\mu}{L} \end{bmatrix} = (\text{displacement vector}) \dots\dots\dots(3)$$

So, the final 3-D TSM of B-C element in local coordinates is:

$$t = \frac{EI}{L} \begin{bmatrix} \zeta_3 \bar{C}_{13} + \frac{\bar{G}_{13} \bar{G} \bar{N}_{13}}{\bar{H}_{13}} & \zeta_3 \bar{C}_{23} + \frac{\bar{G} \bar{N}_{13} \bar{G}_{23}}{\bar{H}_{23}} & \frac{\bar{G} \bar{N}_{13} \bar{G}_{12}}{\bar{H}_{12}} & \frac{\bar{G} \bar{N}_{13} \bar{G}_{22}}{\bar{H}_{22}} & SSG \bar{N}_{13} & \frac{\bar{G} \bar{N}_{13}}{\bar{H}} \\ \zeta_3 \bar{C}_{23} + \bar{G} \bar{N}_{13} \frac{\bar{G}_{23}}{\bar{H}_{23}} & \zeta_3 \bar{C}_{13} + \bar{G} \bar{N}_{23} \frac{\bar{G}_{23}}{\bar{H}_{23}} & \frac{\bar{G} \bar{N}_{23} \bar{G}_{12}}{\bar{H}_{12}} & \frac{\bar{G} \bar{N}_{23} \bar{G}_{22}}{\bar{H}_{22}} & SSG \bar{N}_{23} & \frac{\bar{G} \bar{N}_{23}}{\bar{H}} \\ \frac{\bar{G} \bar{N}_{13} \bar{G}_{12}}{\bar{H}_{12}} & \frac{\bar{G} \bar{N}_{23} \bar{G}_{12}}{\bar{H}_{12}} & \zeta_2 \bar{C}_{12} + \bar{G} \bar{N}_{12} \frac{\bar{G}_{12}}{\bar{H}_{12}} & \zeta_2 \bar{C}_{22} + \bar{G} \bar{N}_{12} \frac{\bar{G}_{22}}{\bar{H}_{22}} & SSG \bar{N}_{12} & \frac{\bar{G} \bar{N}_{12}}{\bar{H}} \\ \frac{\bar{G} \bar{N}_{13} \bar{G}_{22}}{\bar{H}_{22}} & \frac{\bar{G} \bar{N}_{23} \bar{G}_{22}}{\bar{H}_{22}} & \zeta_2 \bar{C}_{22} + \frac{\bar{G} \bar{N}_{12} \bar{G}_{22}}{\bar{H}_{22}} & \zeta_2 \bar{C}_{12} + \bar{G} \bar{N}_{22} \frac{\bar{G}_{22}}{\bar{H}_{22}} & SSG \bar{N}_{22} & \frac{\bar{G} \bar{N}_{22}}{\bar{H}} \\ SSG \bar{N}_{13} & SSG \bar{N}_{23} & SSG \bar{N}_{12} & SSG \bar{N}_{22} & \frac{C_t}{EI} + SS^2 & \frac{SS}{\bar{H}} \\ \frac{\bar{G} \bar{N}_{13}}{\bar{H}} & \frac{\bar{G} \bar{N}_{23}}{\bar{H}} & \frac{\bar{G} \bar{N}_{12}}{\bar{H}} & \frac{\bar{G} \bar{N}_{22}}{\bar{H}} & \frac{SS}{\bar{H}} & \frac{\pi^2}{\bar{H}} \end{bmatrix} \dots\dots\dots(4)$$

$$\left( \bar{G}_{13} = 2\bar{b}_{13}(\theta_{13} + \theta_{23}) + 2\bar{b}_{23}(\theta_{13} - \theta_{23}) + \frac{r}{L}\phi\bar{t}_{13} = \frac{\partial \delta_6}{\partial u_1} / EAL \right) \dots\dots\dots (5)$$

$$\left( \bar{G}_{23} = 2\bar{b}_{23}(\theta_{13} + \theta_{23}) + 2\bar{b}_{13}(\theta_{13} - \theta_{23}) + \frac{r}{L}\phi\bar{t}_{23} = \frac{\partial \delta_6}{\partial u_2} / EAL \right) \dots\dots\dots (6)$$

$$\left( \bar{G}_{12} = 2\bar{b}_{12}(\theta_{12} + \theta_{22}) + 2\bar{b}_{22}(\theta_{12} - \theta_{22}) + \frac{r}{L}\phi\bar{t}_{12} = \frac{\partial \delta_6}{\partial u_3} / EAL \right) \dots\dots\dots (7)$$

$$\left( \bar{G}_{22} = 2\bar{b}_{22}(\theta_{12} + \theta_{22}) + 2\bar{b}_{12}(\theta_{12} - \theta_{22}) + \frac{r}{L}\phi\bar{t}_{22} = \frac{\partial \delta_6}{\partial u_4} / EAL \right) \dots\dots\dots (8)$$

$$\bar{H} = \frac{\pi^2}{\lambda^2} + \frac{1}{\zeta_3} \left( \bar{b}'_{13}(\theta_{13} + \theta_{23})^2 + \bar{b}'_{23}(\theta_{13} - \theta_{23})^2 + \frac{r\phi}{L}(\bar{t}'_{13}\theta_{13} + \bar{t}'_{23}\theta_{23}) \right) + \dots\dots\dots (9)$$

$$\frac{1}{\zeta_2} \left( \bar{b}'_{12}(\theta_{12} + \theta_{22})^2 + \bar{b}'_{22}(\theta_{12} - \theta_{22})^2 + \frac{r\phi}{L}(\bar{t}'_{12}\theta_{12} + \bar{t}'_{22}\theta_{22}) \right)$$

$$(\bar{GN}_{13} = \bar{C}'_{13}\theta_{13} + \bar{C}'_{23}\theta_{23}) \dots\dots\dots (10)$$

$$(\bar{GN}_{23} = \bar{C}'_{23}\theta_{13} + \bar{C}'_{13}\theta_{23}) \dots\dots\dots (11)$$

$$(\bar{GN}_{12} = \bar{C}'_{12}\theta_{12} + \bar{C}'_{22}\theta_{22}) \dots\dots\dots (12)$$

$$(\bar{GN}_{22} = \bar{C}'_{22}\theta_{12} + \bar{C}'_{12}\theta_{22}) \dots\dots\dots (13)$$

$$\bar{H}_{13} = \frac{\pi^4}{\lambda^2} + \frac{1}{\zeta_3} \left[ \bar{b}'_{13}(\theta_{13} + \theta_{23})^2 + \bar{b}'_{23}(\theta_{13} - \theta_{23})^2 + \frac{r}{L}\phi\bar{t}'_{13} \right] \dots\dots\dots (14)$$

$$\bar{H}_{23} = \frac{\pi^4}{\lambda^2} + \frac{1}{\zeta_3} \left[ \bar{b}'_{13}(\theta_{13} + \theta_{23})^2 + \bar{b}'_{23}(\theta_{13} - \theta_{23})^2 + \frac{r}{L}\phi\bar{t}'_{23} \right] \dots\dots\dots (15)$$

$$\bar{H}_{12} = \frac{\pi^4}{\lambda^2} + \frac{1}{\zeta_2} \left[ \bar{b}'_{12}(\theta_{12} + \theta_{22})^2 + \bar{b}'_{22}(\theta_{12} - \theta_{22})^2 + \frac{r}{L}\phi\bar{t}'_{12} \right] \dots\dots\dots (16)$$

$$\bar{H}_{22} = \frac{\pi^4}{\lambda^2} + \frac{1}{\zeta_2} \left[ \bar{b}'_{12}(\theta_{12} + \theta_{22})^2 + \bar{b}'_{22}(\theta_{12} - \theta_{22})^2 + \frac{r}{L}\phi\bar{t}'_{22} \right] \dots\dots\dots (17)$$

$$\left( SS = \text{New factor} = -\frac{r}{L}(\bar{t}_{13}\theta_{13} + \bar{t}_{23}\theta_{23} + \bar{t}_{12}\theta_{12} + \bar{t}_{22}\theta_{22}) \frac{\pi^2}{\lambda^2} \right) \dots\dots\dots (18)$$

$$\left( \zeta_3 = I_3/I, \zeta_2 = I_2/I \right) \dots\dots\dots(19)$$

$$\left( \lambda = L/\sqrt{I/A} \right)$$

$$\left. \begin{array}{l} \left( \bar{C}_{12}, \bar{C}_{22}, \bar{C}_{13}, \bar{C}_{23} : \text{Stability functions including shear deformation} \right) \\ \left( \bar{b}_{12}, \bar{b}_{22}, \bar{b}_{13}, \bar{b}_{23} : \text{New bowing functions including shear deformation} \right) \\ \left( \bar{t}_{12}, \bar{t}_{22}, \bar{t}_{13}, \bar{t}_{23} : \text{New twisting functions including shear deformation} \right) \end{array} \right\} [14]$$

$C_t$ : is the effect of axial force on torsional stiffness

1. For  $C_w \neq 0$  and  $(GJ - \bar{K}) > 0$

$$\therefore C_t = \frac{GJ - \bar{K}}{\left( 1 - \frac{2}{KL} \tanh \frac{KL}{2} \right)} \dots\dots\dots(20)$$

$$K = \sqrt{\frac{1}{EC_w} (GJ - \bar{K})} \dots\dots\dots(21)$$

2. For  $C_w \neq 0$  and  $(GJ - \bar{K}) < 0$

$$\therefore C_t = \frac{GJ - \bar{K}}{\left( 1 - \frac{2}{KL} \tan \frac{KL}{2} \right)} \dots\dots\dots(22)$$

$$K = \sqrt{\frac{1}{EC_w} (\bar{K} - GJ)} \dots\dots\dots(23)$$

3. For  $C_w = 0$

$$\therefore C_t = GJ - \bar{K} \dots\dots\dots(24)$$

Where: -

$$\bar{K} = \text{Wagner Effect} = Pr_0^2$$

$P = \text{axial force}$

$r_0 = \text{Polar Radius of gyration}$

While the uncoupled TSM in space Kassimali & Abbasnia[8]

$$t = \frac{EI}{L} \begin{bmatrix} \zeta_3 C_{13} + \frac{G_{13}^2}{\pi^2 H} & \zeta_3 C_{23} + \frac{G_{13} G_{23}}{\pi^2 H} & \frac{G_{13} G_{12}}{\pi^2 H} & \frac{G_{13} G_{22}}{\pi^2 H} & 0 & \frac{G_{13}}{H} \\ \zeta_3 C_{23} + G_{13} \frac{G_{23}}{\pi^2 H} & \zeta_3 C_{13} + \frac{G_{23}^2}{\pi^2 H} & \frac{G_{23} G_{12}}{\pi^2 H} & \frac{G_{23} G_{22}}{\pi^2 H} & 0 & \frac{G_{23}}{H} \\ \frac{G_{13} G_{12}}{\pi^2 H} & \frac{G_{23} G_{12}}{\pi^2 H} & \zeta_2 C_{12} + \frac{G_{12}^2}{\pi^2 H} & \zeta_2 C_{22} + \frac{G_{12} G_{22}}{\pi^2 H} & 0 & \frac{G_{12}}{H} \\ \frac{G_{13} G_{22}}{\pi^2 H} & \frac{G_{23} G_{22}}{\pi^2 H} & \zeta_2 C_{22} + \frac{G_{12} G_{22}}{\pi^2 H} & \zeta_2 C_{12} + \frac{G_{22}^2}{\pi^2 H} & 0 & \frac{G_{22}}{H} \\ 0 & 0 & 0 & 0 & \frac{C_t}{EI} & 0 \\ \frac{G_{13}}{H} & \frac{G_{23}}{H} & \frac{G_{12}}{H} & \frac{G_{22}}{H} & 0 & \frac{\pi^2}{H} \end{bmatrix} \dots\dots\dots (25)$$

$$G_{13} = C'_{13}\theta_{13} + C'_{23}\theta_{23} \dots\dots\dots (26)$$

$$G_{23} = C'_{23}\theta_{13} + C'_{13}\theta_{23}$$

$$G_{12} = C'_{12}\theta_{12} + C'_{22}\theta_{22} \dots\dots\dots (27)$$

$$G_{22} = C'_{22}\theta_{12} + C'_{12}\theta_{22}$$

$$H = \frac{\pi^2}{\lambda^2} + \sum_{j=1,2} \frac{1}{\zeta_j} \left[ b'_{1j}(\theta_{1j} + \theta_{2j})^2 + b'_{2j}(\theta_{1j} - \theta_{2j})^2 \right] \dots\dots\dots (28)$$

$C_1 =$   
Stability function ( $u=0$ ), [3&14]

$C_2 =$

The TSM in global coordinates is given by Oran[12]:

$$T.S.M = R\bar{B}t\bar{B}^T R^T + \sum_{K=1}^6 \bar{S}_K R\bar{g}^{(K)} R^T \dots\dots\dots (29)$$

### 3- Computational techniques and Program Algorithm:

Many numerical methods and computational techniques are adopted in the present formulation of the new coupled TSM for the beam-column element plus the cable element in space. Cholesky factorization solving technique and the widely known Newton-Raphson incremental, iterative and incremental-iterative mixed methods are used in this work.

The Multi-Purpose Computer Program *NASCFI*: The *NASCFI* (Non-linear Analysis of Space Cable-Frame Interaction structures) program introduces many services. It is capable of handling many types of analyses starting from the linear first order up to the non-linear analysis with all the non-linearities mentioned already. *NASCFI* is developed in the present study to carry out the large

displacement elastic stability static analysis of 2-D and 3-D cable-frame interaction structures as well as of ordinary structures. These include neglecting all types of non-linearities (i.e. first order stability analysis), SD geometrical non-linear analysis without axial effect (second order analysis), LD geometrical non-linear analysis (axial and change in geometry), LD geometrical non-linear analysis with bowing effect excluding the shear and the twisting effects, LD geometrical non-linear analysis including the coupled actions of both bowing and twisting effects but excluding the shear effects, LD geometrical non-linear analysis including the coupled actions of both bowing and twisting effects plus 2 methods of shear effect (the total angle shear effect and the flexural-angle shear effect), the geometrical non-linear buckling analysis (the pre and post buckling critical loads adopting the load control technique and convergence criterion described later), and finally, both cable-frame as well as ordinary structures can be analyzed.

Since this program deals with interaction between cable and beam- column elements, the types of computational techniques mentioned earlier (*N-R*, iterative, incremental and mixed) must be taken into account to satisfy the equilibrium equations. In addition, the tolerance must be achieved for the unbalanced load induced by these techniques at each load level. *NASCFI* follows the following algorithm path:

1. Read the input data: read the nature of structure (either cable-frame or ordinary structure). Then read nature of analysis ( 2-D or 3-D, type of geometrical non-linearity, including shear deformations or not (method indicator, either Meth. -0-, Meth. -1- or Meth. -2-), and finally is it large or small deformation analysis (LD or SD).
2. Using the latest available values for all geometric and static quantities determine the "t" matrix of all elements: read the structural data (properties, geometry and FEA with their " $\Delta P$ ") and initial cable tensions, assume tolerance  $\leq 0.01$ .. Then set all  $\bar{C}_1, \bar{C}_2, \bar{b}_1, \bar{b}_2, \bar{t}_1$  &  $\bar{t}_2$  values at load parameter ( $\rho = 0$ ), and then find " $E_{eq}$ ", [14].
3. Compute " $\tau_y$ " for global coordinates, then assemble the system TSM thus obtained to establish the incremental equations of equilibrium.

4. Solve the equilibrium equations, by substituting " $\tau$ " and " $\Delta P$ " and solving for " $\Delta X$ ", using the Cholesky factorization method.
5. Determine the new geometric configuration of the structure.
  - a. Determine the new joint locations (coordinates) from:

$$\{X\}_{i+1} = \{X\}_i + \{\Delta X\}_i \dots\dots\dots(30)$$

Note that the translation components of  $\{X\}_{i+1}$  determine the new locations of all joints of the system while the rotation components  $\{X\}_{i+1}$  do not have a well defined physical significance, e.g. cumulative values are calculated exclusively for use in the convergence criteria described subsequently.

- b. Determine the new joint orientation matrix for each joint:
  - I. For each member, determine:

$$\{\Delta \bar{v}\} = [R]^T \{\Delta v\}, \{\Delta u\} = [\bar{B}]^T \{\Delta \bar{v}\} \dots\dots\dots(31)$$

$$\{u + \Delta u\} \dots\dots\dots(32)$$

$$\{S + \Delta S\} = [t]\{u + \Delta u\} \dots\dots\dots(33)$$

$$\{\Delta r\} = [r][\Delta \bar{\gamma}] \dots\dots\dots(34)$$

$$[r + \Delta r] \dots\dots\dots(35)$$

In which  $[\Delta \bar{\gamma}]$  is the incremental rotation matrix for the member in member coordinates –Eq. (36):

$$[\Delta \bar{\gamma}] = \begin{bmatrix} 0 & -\Delta \bar{\gamma}_3 & \Delta \bar{\gamma}_2 \\ \Delta \bar{\gamma}_3 & 0 & -\Delta \bar{\gamma}_1 \\ -\Delta \bar{\gamma}_2 & \Delta \bar{\gamma}_1 & 0 \end{bmatrix} \dots\dots\dots(36)$$

$$\Delta \bar{\gamma}_1 = \frac{1}{2}(\Delta \bar{v}_4 + \Delta \bar{v}_{10}) \dots\dots\dots(37)$$

$$\Delta \bar{\gamma}_2 = \Delta \bar{v}_3 - \Delta \bar{v}_9 \dots \dots\dots(38)$$

$$\Delta \bar{\gamma}_3 = -\Delta \bar{v}_2 + \Delta \bar{v}_8 \dots \dots\dots(39)$$

- II. For each member determine: -

$$[\Delta \alpha] = [\Delta W][\alpha] \dots\dots\dots(40)$$

$$[\alpha + \Delta\alpha] \dots \dots \dots (41)$$

In which  $[\Delta W]$  is the incremental rotation matrix for the member in global coordinates –Eq. (42):

$$[\Delta W] = \begin{bmatrix} 0 & -\Delta W_3 & \Delta W_2 \\ \Delta W_3 & 0 & -\Delta W_1 \\ -\Delta W_2 & \Delta W_1 & 0 \end{bmatrix} \dots \dots \dots (42)$$

and:

$$\Delta W_1 = \begin{bmatrix} \text{either } \Delta v_4 \\ \text{or } \Delta v_{10} \end{bmatrix} \dots \dots \dots (43)$$

$$\Delta W_2 = \begin{bmatrix} \text{either } \Delta v_5 \\ \text{or } \Delta v_{11} \end{bmatrix} \dots \dots \dots (44)$$

$$\Delta W_3 = \begin{bmatrix} \text{either } \Delta v_6 \\ \text{or } \Delta v_{12} \end{bmatrix} \dots \dots \dots (45)$$

Depending on the particular joint under consideration, all other quantities are defined in the derivation of the uncoupled TSM in space for the technique proposed by others[8], [10], &[12].

6. Determine member end forces. Firstly, for each member the end forces " $\bar{S}$ " are determined, and then the end forces in global coordinates ( $\bar{F} = R\bar{B}\bar{S}$ ). In this step the computational difficulty of the axial force is induced from the relative member deformations (see remark B).
7. The solution obtained thus far represents an approximate configuration in the sense that the system equilibrium equations are not necessarily satisfied at the load level " $P_{i+1}$ ". This approximate solution is corrected by a *N-R* types detailed earlier until the equilibrium equations are satisfied within a prescribed tolerance. In the following, the subscript "*j*" refers to the "*j*<sup>th</sup>" iteration cycle, while "*P*" is kept constant at " $P_{i+1}$ ". The unbalanced joint forces, " $\Delta Q$ " are determined from ( $\Delta Q_j = P - f(F_j)$ ).
8. Using the latest available values of all geometric and static quantities determine "*t*" in local coordinates, then for each member TSM in global coordinates, then assemble the system TSM. For the cable element, determine the secant equivalent modulus of elasticity, and then use it in calculating the new "*t*" matrix of this element, then establish its TSM ( $\tau$ ).

9. Treating the unbalanced joint forces as a load increment, determine the correction factor, " $\Delta X$ " from the incremental relationship:

$$[\tau]_j \{\Delta X\}_j = \{\Delta Q\}_j \dots \dots \dots (46)$$

10. If the correction displacement vector is not small enough, determine the new joint locations: -

a.  $\{X\}_{j+1} = \{X\}_j + \{\Delta X\}_j \dots \dots \dots (47)$

b. New joint orientation matrix

Then repeat steps from "5" to "10" until the " $\Delta X$ " value is sufficiently small according to a prescribed criterion (see *remark A*).

11. Consider a new load increment, " $\Delta P$ ", and return to step "2".

*Remark A:* The specific displacement convergence criterion used herein is given by:

$$\left[ \frac{\sum_1 (\Delta X)_i^2}{\sum_1 (X)_i^2} \right] \leq e \dots \dots \dots (48)$$

"e" is a prescribed tolerance. In applying this criteria, translation and rotation components of-X- are treated as separate groups, and convergence is assumed to have occurred when Eq.(48) is satisfied simultaneously and independently for each group. However, "e" is taken equal to  $(10^{-5})$ .

*Remark B:* In step "6" there will be a difficulty caused by the axial force from relative member deformation in determining  $\bar{s}$  from " $\bar{u}$ ". This is because the expression for member axial force, "Q" as given:

$$Q = EA \left( \frac{u}{L} - C_{b3} - C_{b2} - C_{T3} - C_{T2} \right) \dots \dots \dots (49)$$

"Q" Involves bowing and twisting functions ( $\bar{b}_{1j}, \bar{b}_{2j}, \bar{t}_{1j}$  &  $\bar{t}_{2j}$ ) which in turn are functions of axial force parameter " $\rho$ ". This problem can be solved using an iteration technique[7]:

$$K(\rho) = \frac{\pi^2}{\lambda^2} \rho - \frac{u}{L} + C_{b3} + C_{b2} + C_{T3} + C_{T2} = 0 \dots \dots \dots (50)$$

Let  $\rho_1$  be an approximate solution of this equation. By using a first order Taylor series expansion[7]:

$$K(\rho_i + \Delta\rho_i) = K(\rho_i) + K'(\rho_i)\Delta\rho_i = 0 \dots\dots\dots(51)$$

In which a prime superscript denotes a differentiation with respect to  $\rho$ , and: -

$$K'(\rho) = \frac{\pi^2}{\lambda^2} + C'_b + C'_T \dots\dots\dots(52)$$

An approximate solution, ( $\rho_i$ ) of eq.(51) is initially assumed, and is modified successively by using relationship:-

$$\rho_{i+1} = \rho_i + \Delta\rho_i = \rho_i - \frac{K(\rho_i)}{K'(\rho_i)} \dots\dots\dots(53)$$

Where:

$$K'(\rho_i) = \frac{dK(\rho)}{d\rho} = \bar{H} \dots\dots\dots(54)$$

" $\bar{H}$ " is taken from Eq.(9)

This iteration continues till " $\Delta\rho < e$ ", where "e" is taken as a prescribed tolerance equal to (0.001).

$$C'_b = b'_1(\theta_1 + \theta_2)^2 + b'_2(\theta_1 - \theta_2)^2 + 2b_1(\theta_1 + \theta_2)(\theta'_1 + \theta'_2) + 2b_2(\theta_1 - \theta_2)(\theta'_1 - \theta'_2) \dots\dots\dots(55)$$

$$C'_T = \frac{rM_t}{(GJ + \bar{K})}(\bar{t}'_1\theta_1 + \bar{t}'_2\theta_2 + \bar{t}_1\theta'_1 + \bar{t}_2\theta'_2)$$

The prime superscript of the angle ( $\theta$ ) can be classified into two groups: -

I The rigidly connected joints, where the rotations at such rigid ends are defined by the global joint displacement and remain constant during this iteration process.

$$\theta_i = 0 \dots\dots\dots(56)$$

II The pinned connected joints, the values of the angles ( $\theta_i$ ) and their derivatives ( $\theta'_i$ ) as follows:

a- End-1- is hinged: -

$$\theta_1 = \frac{C_2}{C_1}\theta_2 \dots\dots\dots(57)$$

$$\theta'_1 = \frac{\theta_2}{C_1^2}(C'_1C_2 - C_1C'_2) \dots\dots\dots(58)$$

b- End-2- is hinged: -

$$\theta_2 = \frac{C_2}{C_1} \theta_1 \dots\dots\dots(59)$$

$$\theta'_2 = \frac{\theta_1}{C_1^2} (C'_1 C_2 - C_1 C'_2) \dots\dots\dots(60)$$

c- Both ends are hinged:-

$$\theta_1 = -\theta_2 \text{ for first buckling mode } \dots\dots\dots(61)$$

$$\theta_1 = \theta_2 \text{ for second buckling mode } \dots\dots\dots(62)$$

After determining the axial force, "Q", by the iterative procedure, member end moments are then computed from:

$$M_{1j} = \frac{EI_j}{L} (\bar{C}_{1j} \theta_{1j} + \bar{C}_{2j} \theta_{2j}) \dots\dots\dots(63)$$

$$M_{2j} = \frac{EI_j}{L} (\bar{C}_{2j} \theta_{1j} + \bar{C}_{1j} \theta_{2j}) \dots\dots\dots(64)$$

$$M_t = \frac{C_t}{L} \phi_t \dots\dots\dots(65)$$

$$Q = EA \left( \frac{u}{L} - C_{b_3} - C_{b_2} - C_{T_3} - C_{T_2} \right) \dots\dots\dots(66)$$

Where j=2, 3.

This program is coded using *FORTRAN77* language with *LAHEY* compiler on an IBM-PC computer.

## 4- Numerical Examples

Three different examples are checked by *NASCFI* using the coupled TSM and compared with previous uncoupled solutions.

### 4.1 Case Study No. 1: 3-D Initial Imperfection Circular Ring Pin-Ended Beam-Column:

This problem was analyzed by many investigators using elastic-plastic analysis as shown in Table 1.b. Three cases are studied for this problem:  $L/r_0 = 80, 120, \& 160$ , respectively. The properties of

all cases are detailed in Table 1.a. This analysis involved elastic and elastic-plastic behavior covering both material and geometrical non-linearities. The usual technique used in analyzing this problem was the finite segment method assuming the generalized cyclic stress-strain relationship for the material non-linearity and an automatic load-control technique with an initial central deflection of  $0.001L$  being assumed.

Table 1.b illustrates all the previous attempts in analyzing this problem, in addition to the present three methods of shear effect (Meth. -0-, -1-, & -2-). Although the work done before was elastic-plastic analysis, the portion concerning this work deals with pre-buckling stability analysis which is actually elastic. Thus the comparison is done in this portion only with a recommendation that an elastic-plastic development on the present study is to be done in the future. The "u" value is taken constant in both horizontal directions since the same Poisson's ratio " $\nu = 0.5$ " and shape factor "n" for circular section are used.

In Figs. 1.a, 1.b, and 1.c, it can be observed clearly that the shear effect in three cases is negligible in both SD and LD analysis. Nevertheless, the higher  $L/r_0$  the lower the differences between Meth. -0- and shear including methods Meth. -1- & Meth. -2-. This is due to the simple fact that the "u" value depends on the  $L/r_0$  value, as it is obvious from the definition of the shear parameter "u" (see App. II).

Furthermore, the larger the  $L/r_0$  value the higher the divergence between SD and LD results. This is simply because of the reason that whenever the member or the element gets longer or more slender the LD effects will be more considerable and effective. Both Table 1 and Fig. 1 show good agreement between the present formulation and that by others elastic results.

The higher  $L/r_0$  the higher the new twisting effect observed as the SS/SS0 ratio for the three cases indicate. These are 2.83%, 3.46%, and 5.58% increment respectively for both methods. Where (SS) indicates including the new twisting effects, while (SS0) indicates disregarding it. In the SD analysis the ratio SS/SS0 equals (1) in the three cases, which insure the fact that the new effect is considerable only in the LD analysis.

## 4.2 Case No. 2: 3-D Cantilever Horizontal Bent Joint

Kassimali and Abbasnia[8] have shown that the numerical results of this problem nearly coincide by taking 2 elements or 4 elements, except for  $X_3$ - direction. The properties of this problem are given in Table 2.a. Table 2.b summarizes the work by others and their comparison with the present analytical results. Fig. 2 illustrates the P- $\Delta$  behavior of this problem in the directions  $X_1$  and  $X_3$ . It can easily be recognized that there is a great deal of coincidence, between this work and Kassimali and Abbasnia[8]. Since Meth. -0- & Meth. -1- and Meth. -2- lead to identical paths, i.e. the shear effect is insignificant.

At 8.9 kN the SD/LD divergence are 0.935 for  $X_1$  direction, 1.141 for  $X_2$  direction, and 0.913 in  $X_3$  direction respectively. No instability has been noticed in this case study. When the bowing terms were neglected, convergence could not be achieved for the two elements modeled at the first load step  $P=0.89$  kN. This agrees with the study of Kassimali and Abbasnia[8].

The SS/SS0 exhibits 5.896% increment for  $X_1$ , and 5.619% drop for  $X_2$  for both methods. This confirms the validity of *the new theoretical approach and the new coupled TSM*. Also the SS/SS0 equals to (1) when used the SD analysis.

## 4.3 Case Study No. 3: Framed Dome With Vertical Load

For further validation 3-D example of an imperfect sensitive 18-member frame dome shown in Fig. 3.a. This was analyzed by many researchers as shown in Table 3.b. Table 3.a indicates the properties and load condition of the problem. A single load is applied at the top joint or crown of the dome.

Fig. 3.b shows the excellent convergence between the present formulation and the other efforts in both pre-buckling and post-buckling regions of the curve. Although the "u" value is increased in comparison with the earlier cases, it can be found that the shear effect is still insignificant in the stability analysis of the structures. Also at 89 MN the ratio SD/LD divergence is about 1.1208, while the ratio SS/SS0 is 5.77% drop using the LD analysis.

## 5. CONCLUSIONS

1. The new coupled TSM introduces a significant difference with the old uncoupled TSM.
2. For the beam-column case studies, *NASCFI* shows good agreement of the new approach with exact large Elastica solved problems or with the experimental problems.
3. Including new effects of both (the flexural-shear bowing and the 3-D effect) the present work indicates a significant amount of difference with other research results of the corresponding problems.
4. The new twisting effect has a major role that relates the axial deformation with the shear effect acting transversely.

## APPENDIX I: REFERENCES

1. **Al-Rawanduzy, A. A., 1996.** Large Displacement Elastic Stability Analysis of Plane Steel Frames and Dynamic Loads. MSc. thesis, Building and Construction Engineering Department, University of Technology, Baghdad-Iraq, pp.67-120.
2. **Al-Sadder, S.Z.R., 1994.** Large Displacement Elastic-Plastic Stability Analysis of Plane Steel Frames with Non - Linear Connections. MSc. thesis, Civil Engineering Department, University of Baghdad, Baghdad-Iraq, pp. 5-40.
3. **Al-Sarraf, S. Z., 1986.** Shear Effect on the Elastic Stability of Frames, The Structural Engineer Journal, Vol. 64B, No. 2, pp.43-47.
4. **Borri, C. and S. Chostrini, 1989.** Non-Linear Approach to the Stability Analysis of Space Beam Structures. International Journal of Space Structures, Vol. 4 No. 4, 193-220.
5. F77L-EM/32, FORTRAN LANGUAGE SYSTEM REFERENCE MANUAL, Revision B (1989), Lahey Computer Systems, Inc., Incline Village, NV 89450-6091, USA.

6. **Gere and Weaver, 1963.** Analysis of Framed Structures. New York - U.S.A., D. Van Nostrand Company, , pp.108-300.
7. **Kassimali W. A., 1983.** Large Deformation Analysis of Elastic-Plastic Frames. Journal of Structural Engineering ASCE, Vol. 109, No.8, pp.1869-1887.
8. **Kassimali W. A., and R. Abbasnia, 1991.** Large Deformation Analysis of Elastic Space Frames. Journal of Structural Engineering ASCE, Vol. 117, No. 7, pp.2069-2087.
9. **Noor, A. K., 1974.** Non-Linear Analysis of Space Truss. Journal of Structural Division, ASCE., Vol. 100, No. ST3, pp.533-546.
10. **Oran, C. and A. Kassimali, 1976.** Large Deformation of Framed Structures Under Static and Dynamic Loads. International Journal of Computers and Structures, Vol.6, pp.539-547.
11. **Oran, C., 1973.** Tangent Stiffness in Plane Frames. Journal of Structural Division, ASCE, Vol. 99, No. ST6, pp. 973-985.
12. **Oran, C., 1974.** Tangent Stiffness in Space Frames. Journal of Structural Division, ASCE, Vol. 100, No. ST7, pp.1473-1487.
13. **Saffan, S. A., 1963.** Non-Linear Behavior of Structural Plane Frames. Journal of Structural Division, ASCE, Vol.89, No. ST4, pp. 557-579.

14. **Sideek, K.F., 1997.** Shear and 3-D deformation effects on the stability of elastic cable-stayed towers under static loads. Ph.D. thesis, University of Technology, Baghdad-Iraq, pp. 38-197.
  
15. **Timoshenko and Goodier, 1970.** Theory of Elasticity. New York - U.S.A., McGraw-Hill Book Co., Inc., 3rd Edition, , pp. 291-324.
  
16. **Timoshenko, S. P. and Gere, J. M., 1961.** Theory of Elastic Stability. New York - U.S.A. McGraw-Hill Book Co., Inc., 2nd Edition, , pp.76-142.

**APPENDIX II: NOTATIONS:** The following symbols are used in this paper:

A	Area of section
$A_w$	Web area
$b_1, b_2$	First & second bowing function for no shear effect respectively.
$C_1, C_2$	First & second stability function for no shear effect respectively.
$C_b$	Bowing factor for no shear effect
$C_t$	Axial force effect on torsional rigidity
CT	Twisting factor including shear effect
$C_w$	Warping effect coefficient
E, G	Elastic modulus & shear modulus respectively.
$I_0, J$	Polar moment of inertia of section
L	Original length
$L_c$	Updated length
M	End moment
n	Shape factor
P	Axial force

$P_{cr}, P_e$	Critical axial load & Euler load respectively.
$R$	Radius of curvature
$r$	Radius of section
$r_0$	Radius of gyration
$s$	Arc length
$u$	Shear parameter $\left( u = \frac{nP_e}{AG} = \frac{2n(1+\nu)\pi^2}{(L/r_0)^2} \right)$ for solid cross section
$V$	Shear force
$W$	Load intensity
$y$	Deflection in 2-D analysis for no shear effect
$\bar{c}_1, \bar{c}_2$	First & second stability function for shear effect respectively.
$\bar{b}_1, \bar{b}_2$	First & second bowing function for shear effect respectively.
$\bar{t}_1, \bar{t}_2$	First & second new twisting function respectively.
$\bar{K}$	Wagner effect
$\bar{C}_b$	Bowing factor including shear effect
$\rho, \bar{\rho}$	Axial force parameters for : no shear effect, & including shear effect respectively.
$\bar{u}, \bar{v}, \bar{w}$	Deflections in the three directions of 3-D analysis
$\bar{y}$	Deflection in 2-D analysis including shear effect
$\theta$	Slope of the elastic curve
$\sigma, \epsilon, \nu$	Axial stress, axial strain, & Poisson's ratio respectively.
$\Phi$	Curvature
$\phi$	Angle of twist
$[\bar{\gamma}]$	Rotational matrix in local coordinates
$[\Delta\bar{\gamma}]$	Incremental rotational matrix in local coordinates

$[\tau]$	Overall TSM for the B-C element in global coordinates
$[\Delta W]$	Incremental rotational matrix in global coordinates
$[r]$	Transformation matrix
$[t]$	Tangent stiffness matrix for the beam-column element for relative deformations.
$[W]$	Rotational matrix in global coordinates
$\{\lambda\}_i, \{\Delta\lambda\}_i$	The load & the incremental load parameter vectors in the $i^{\text{th}}$ load cycle respectively.
$\{\Delta P\}_i$	The incremental applied load vector in the $i^{\text{th}}$ cycle of loading
$\{\Delta Q\}_i$	The incremental load equilibrium vector in the $i^{\text{th}}$ cycle of loading
$\{\Delta X\}_i$	The incremental displacement vector in the $i^{\text{th}}$ cycle of loading
$\{F\}_i$	The nodal force vector in the $i^{\text{th}}$ cycle of loading
$\{P\}_i$	The applied load vector in the $i^{\text{th}}$ cycle of loading
$\{Q\}_i$	The load equilibrium vector in the $i^{\text{th}}$ cycle of loading
$\{X\}_i$	The displacement vector in the $i^{\text{th}}$ cycle of loading

The following abbreviations are used in this paper

B-C	Beam-column
DOF	Degree of freedom
E-P	Elastic-plastic analysis
FEA	Fixed end action.
FEM., FSM	Finite element method & finite segment method, respectively.
LAHEY	F77L-EM/32, FORTRAN 77 compiler on an IBM-PC computer.
Meth. -0-	The no shear effect.
Meth -1-, Meth -2-	The total shear slope & the flexural shear slope approaches respectively.
N-R	Newton-Raphson
SD, LD	Small deflection & large deflection analysis respectively.

SS/SS0	The ratio of including the SS effect to excluding it.
TSM	Tangent stiffness matrix.

## **List of Figures**

Figure (1.a): Load-deflection curve for the 3-D initial imperfection pin-ended circular ring for  $L/r=80$ .

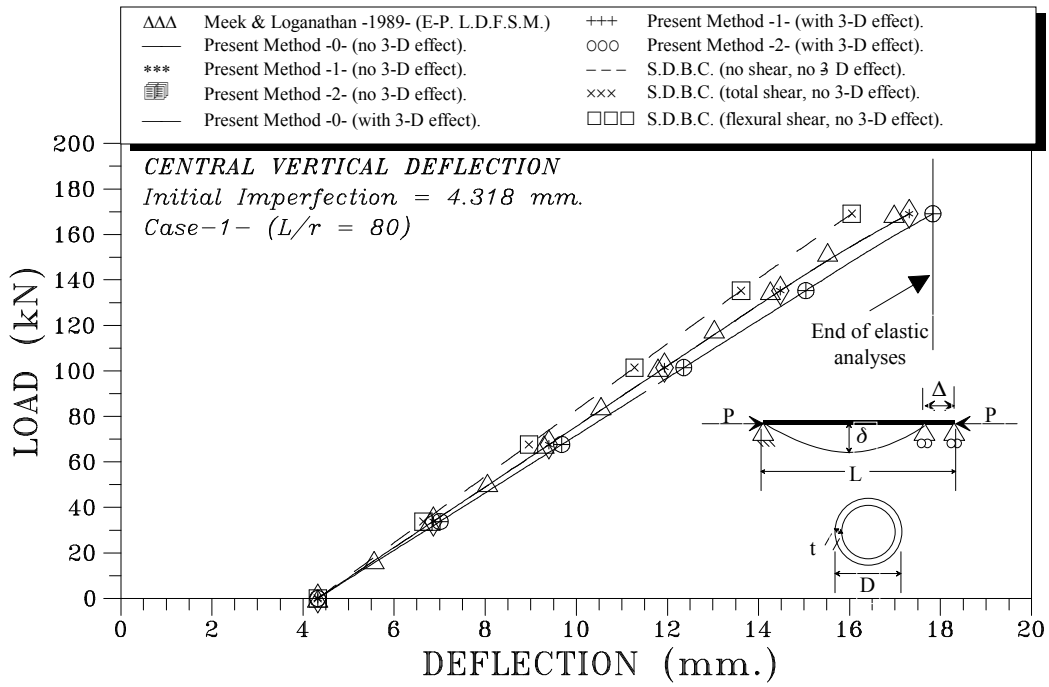
Figure (1.b): Load-Deflection curve for the 3-D initial imperfection pin-ended circular ring for  $L/r=120$ .

Figure (1.c): Load-Deflection curve for the 3-D initial imperfection pin-ended circular ring for  $L/r=160$ .

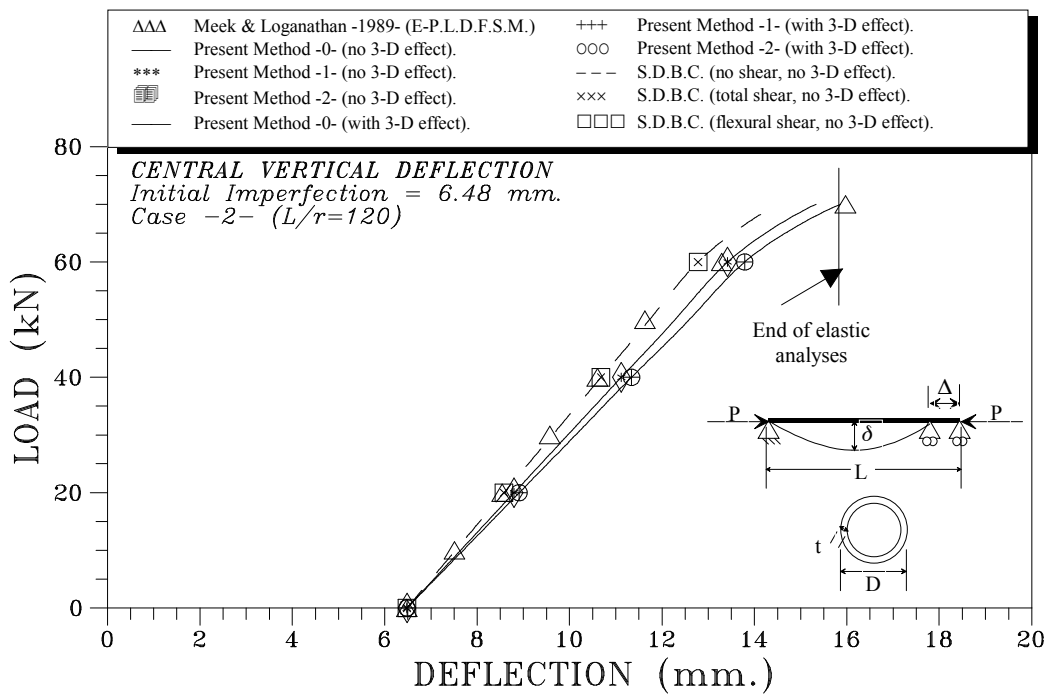
Figure (2): Load-Deflection curve for the 3-D Horizontal bent joint frame.

Figure (3.a): Frame dome with crown load details.

Figure (3.b): Load-deflection curve for the 3-D crown vertical load dome.



**Figure (1.a): Load-deflection curve for the 3-D initial imperfection pin-ended circular ring for  $L/r=80$**



**Figure (1.b): Load-Deflection curve for the 3-D initial imperfection pin-ended circular ring for  $L/r=120$**

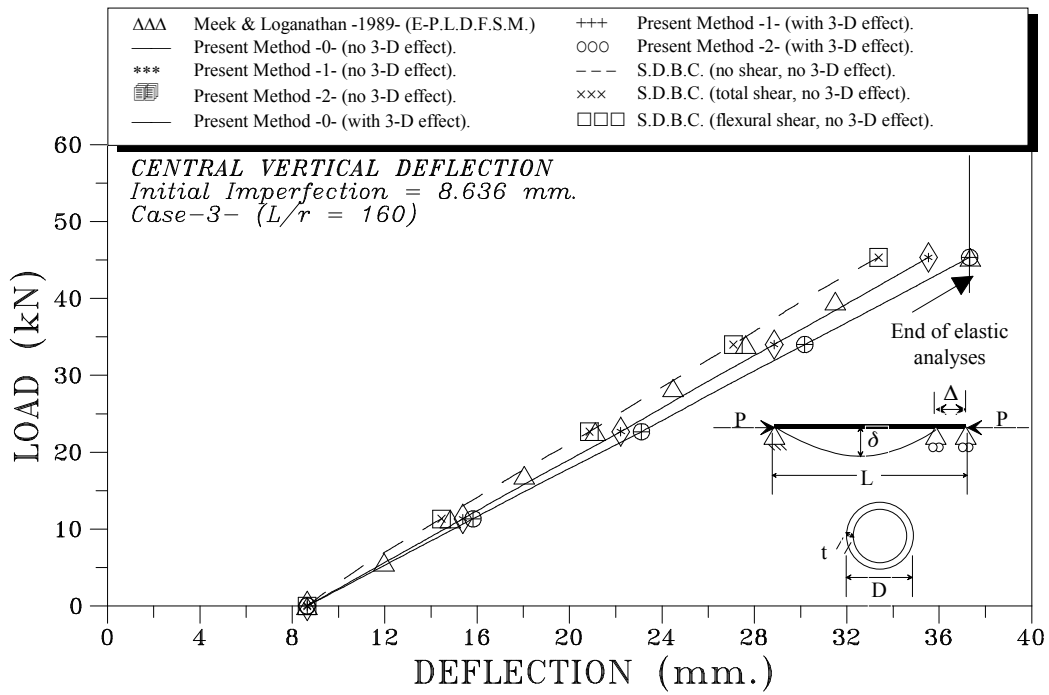


**Figure (1.c): Load-Deflection curve for the 3-D initial imperfection pin-ended circular ring for  $L/r=160$**

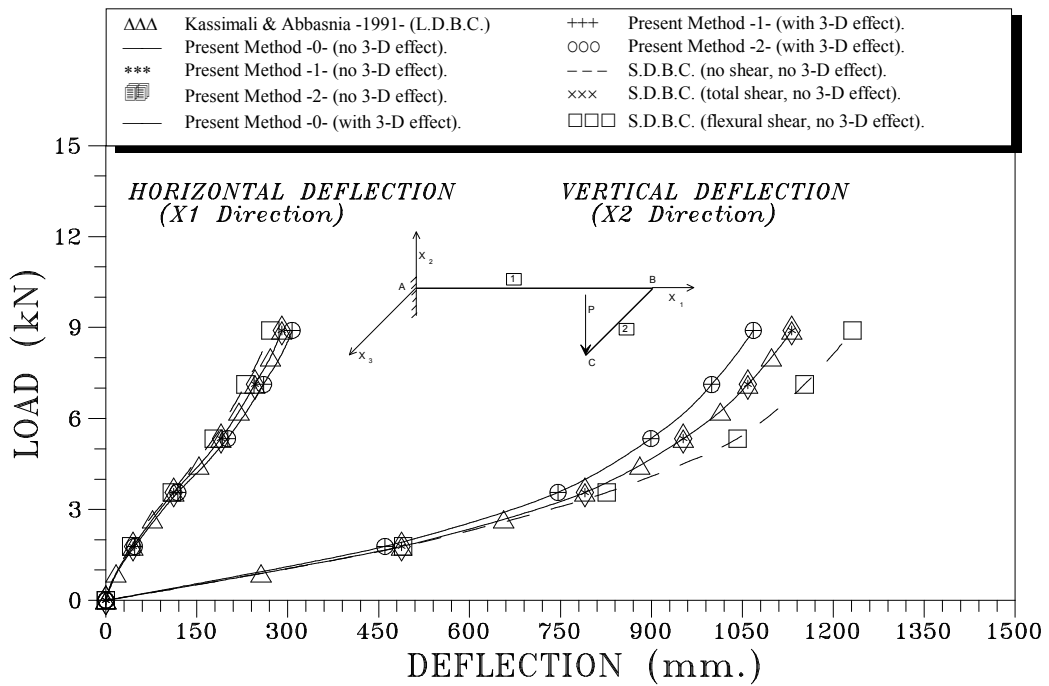


**Figure (2): Load-Deflection curve for the 3-D Horizontal bent joint frame**



**Table 1.a: 3-D Initial Imperfection Circular Ring Pin-Ended Beam-Column Properties**

<i>Case (1)</i>	<i>Element Section D*t(mm.) (2)</i>	<i>L/r<sub>0</sub> (3)</i>	<i>Leng. "L(mm)" (4)</i>	<i>Area "A(mm<sup>2</sup>)" (5)</i>	<i>Moment of Inertia "I(mm<sup>4</sup>)" (6)</i>	<i>Elastic Modulus "Ei(Mpa)" (7)</i>	<i>Initial Imperfection "e<sub>0</sub>/L" (8)</i>	<i>Shear Prmt. "u" (all directions) (9)</i>	<i>Axial Load "P(kN)" (10)</i>
1	114.3*2.38	80	4318	807.095	2351416.2	199955	0.001	0.00513	170.0
2	114.3*2.38	120	6477	807.095	2351416.2	199955	0.001	0.00282	100.0
3	114.3*2.38	160	8636	807.095	2351416.2	199955	0.001	0.00128	57.75

**Table 1.b: Results & Comparison of 3-D Initial Imperfection Circular Ring Pin-Ended Beam-Column**

<i>No. (1)</i>	<i>Method (2)</i>	<i>Type of Analysis (3)</i>	<i>No. of Element (4)</i>	<i>No. of Increment (5)</i>	<i>Central Deflection "(mm.)"</i>		
					<i>Case 1 (6)</i>	<i>Case 2 (7)</i>	<i>Case 3 (8)</i>
1	Sugimoto & Chen (1985)	E-P ,F.S.M. LD	26	10	16.784 at 169.1 kN	15.082 at 70.0 kN	37.341 at 45.336 kN
2	Chan & Kitipornchai (1988)	E-P ,F.S.M. LD	12	16	16.513 at 169.1 kN	15.243 at 70.0 kN	36.953 at 45.336 kN
3	Meek & Loganathan (1989)	E-P ,F.S.M. LD	12	16	16.979 at 169.1 kN	15.973 at 70.0 kN	37.342 at 45.336 kN
4	Present Method "0"	Beam-Col. LD "No Shear"	1	10	17.308 at 169.1 kN	15.330 at 70.0 kN	35.531 at 45.336 kN
5	Present Method "1"	Beam-Col. LD "with Shear"	1	10	17.309 at 169.1 kN	15.330 at 70.0 kN	35.531 at 45.336 kN
6	Present Method "2"	Beam-Col. LD "with Shear"	1	10	17.308 at 169.1 kN	15.330 at 70.0 kN	35.530 at 45.336 kN

**Table 2.a: Two-Member Bent-Joint Frame Properties**

<i>Element</i>	<i>Length</i>	<i>Area</i>	<i>Shear Modulus</i>	<i>Moment of Inertia of 3-Directions</i>			<i>Shear Parameter</i>	<i>Joint Load</i>
				<i>In <math>X_1</math>-Direct</i>	<i>In <math>X_2</math>-Direct</i>	<i>In <math>X_3</math>-Direct</i>		
<i>"(i)"</i>	<i>"<math>L_i</math> (mm)"</i>	<i>"<math>A_i</math>(mm<sup>2</sup>)"</i>	<i>"<math>G_i</math>(Mpa)"</i>	<i>"<math>I_1</math> (mm.<sup>4</sup>)"</i>	<i>"<math>I_2</math> (mm.<sup>4</sup>)"</i>	<i>"<math>I_3</math>(mm.<sup>4</sup>)"</i>	<i>"<math>u_{xi}</math>"</i>	<i>(kN)</i>
<i>(1)</i>	<i>(2)</i>	<i>(3)</i>	<i>(4)</i>	<i>(5)</i>	<i>(6)</i>	<i>(7)</i>	<i>(8)</i>	<i>(9)</i>
1	1524.00	511.3925	80000	41623.14	20811.57	20811.57	X <sub>1</sub> =.00125 X <sub>3</sub> =.00062	0.00
2	254.00	511.3925	80000	41623.14	20811.57	20811.57	X <sub>1</sub> =.04483 X <sub>3</sub> =.02241	8.90

**Table 2.b: - Comparison of Solutions For Two-Member Bent-Joint Frame**

<i>No.</i>	<i>Method</i>	<i>Type of Analysis</i>	<i>No. of Element</i>	<i>No. of Increment</i>	<i>Deflections of Joint -C- in (mm.)</i>		
					<i>Vert. Defl. "<math>x_2</math>"</i>	<i>Horiz. Defl. "<math>x_1</math>"</i>	<i>Horiz. Defl. "<math>x_3</math>"</i>
<i>(1)</i>	<i>(2)</i>	<i>(3)</i>	<i>(4)</i>	<i>(5)</i>	<i>(6)</i>	<i>(7)</i>	<i>(8)</i>
1	Oran (1973)	Beam-Column LD	2	10	1131.73	291.96	-76.225
2	Kassimali & Abbasnia(1990)	Beam-Column LD "with bowing"	2	10	1131.57	290.17	-158.75
3	Present Meth.-0-	Beam-Column LD "no shear"	2	10	1131.57	290.17	-158.75
4	Present Meth.-1-	Beam-Column LD "with shear"	2	10	1131.58	290.18	-158.75
5	Present Meth.-2-	Beam-Column LD "with shear"	2	10	1131.57	290.18	-158.75

**Table 3.a: Framed Dome with Crown Load Properties**

<i>Element "i" (1)</i>	<i>Length "L<sub>i</sub> (mm)" (2)</i>	<i>Area "A<sub>i</sub> (mm<sup>2</sup>)" (3)</i>	<i>Inertia "I<sub>1</sub>(mm<sup>4</sup>)" (4)</i>	<i>Inertia "I<sub>3</sub> (mm<sup>4</sup>)" (5)</i>	<i>Elastic Mod. "E<sub>i</sub> (Mpa)" (6)</i>	<i>Shear Mod. "G<sub>i</sub> (Mpa)" (7)</i>	<i>Shear Parameter "u<sub>xi</sub>" (8)</i>	<i>Equal Joint Load =8 9 MN (9)</i>
1 & 6	1084.2	6451.60	5550029.83	2167872.01	20685	1280	X <sub>1</sub> =0.0260 X <sub>3</sub> =0.0102	
2,3,4 & 5	620.93	6451.60	5550029.83	2167872.01	20685	1280	X <sub>1</sub> =0.0793 X <sub>3</sub> =0.0309	
7,9,10&12	1047.5	6451.60	5550029.83	2167872.01	20685	1280	X <sub>1</sub> =0.0278 X <sub>3</sub> =0.0109	
8 & 11	1047.5	6451.60	5550029.83	2167872.01	20685	1280	X <sub>1</sub> =0.0278 X <sub>3</sub> =0.0109	
14,15,17&18	539.5	6451.60	5550029.83	2167872.01	20685	1280	X <sub>1</sub> =0.1050 X <sub>3</sub> =0.0411	
13&16	1055.5	6451.60	5550029.83	2167872.01	20685	1280	X <sub>1</sub> =0.0274 X <sub>3</sub> =0.0107	

**Table 3.b: Comparison of Solutions For Framed Dome with Crown Load**

<i>No. (1)</i>	<i>Method (2)</i>	<i>Type of Analysis (3)</i>	<i>No. of Element (4)</i>	<i>No. of Increment (5)</i>	<i>Crown Vertical Deflection "mm." (6)</i>
1	Oran (1973)	Beam-Column-LD-	18	22	2636.52 at 89 MN
2	Papadrakakis & Ghionis (1986)	Finit-Element –LD-	48	25	2650.10 at 89 MN
3	Al-Bermani& Kitipornchai (1990)	Beam-Column –LD-	18	25	2647.014 at 89 MN
4	Kassimali & Abbasnia (1990)	Beam-Column-LD "with bowing"	18	22	2651.70 at 89 MN
5	Present Meth.-0-	Beam-Column -LD "no shear"	18	22	2651.73 at 89 MN
6	Present Meth.-1-	Beam-Column- LD "with shear"	18	22	2651.84 at 89 MN
7	Present Meth.-2-	Beam-Column-LD "with shear"	18	22	2651.82 at 89 MN